Cancer Nanotechnology

RESEARCH Open Access

Pristine/folate-functionalized graphene oxide as two intrinsically radioiodinated nano-theranostics: self/dual in vivo targeting comparative study

Mohamed M. Swidan[1], Basma M. Essa[2*] and Tamer M. Sakr[2]

*Correspondence:
basmamohamed24@yahoo.com

[1] Labeled Compounds Department, Hot Laboratories Center, Egyptian Atomic Energy Authority, Cairo 13759, Egypt
[2] Radioactive Isotopes and Generators Department, Hot Laboratories Center, Egyptian Atomic Energy Authority, Cairo 13759, Egypt

Abstract

Background: Nanomedicine offers great potentials for theranostic studies via providing higher efficacy and safety levels. This work aimed to develop and evaluate a new nanoplatform as a tumor theranostic probe.

Results: Carboxyl-functionalized graphene oxide nanosheets (FGO) was well synthesized from graphite powder and then conjugated with folic acid to act as a targeted nano-probe. Full characterization and in vitro cytotoxicity evaluation were conducted; besides, in vivo bio-evaluation was attained via intrinsic radioiodination approach in both normal and tumor-bearing Albino mice. The results indicated that FGO as well as conjugated graphene oxide nanosheets (CGO) are comparatively non-toxic to normal cells even at higher concentrations. Pharmacokinetics of FGO and CGO showed intensive and selective uptake in the tumor sites where CGO showed high T/NT of 7.27 that was 4 folds of FGO at 1 h post injection. Additionally, radioiodinated-CGO (ICGO) had declared a superior prominence over the previously published tumor targeted GO radiotracers regarding the physicochemical properties pertaining ability and tumor accumulation behavior.

Conclusions: In conclusion, ICGO can be used as a selective tumor targeting agent for cancer theranosis with aid of I-131 that has a maximum beta and gamma energies of 606.3 and 364.5 keV, respectively.

Keywords: Graphene oxide nanosheets, Folic acid, Intrinsic radioiodination, Theranostic, Nanoplatform, Tumor, Intrinsic

Background

Currently, various malignancies have greatly influenced and invaded human life, with 14 million new cancer patients annually worldwide, posing a global threat (Jaymand, et al. 2021). The global reluctance towards cancer has promoted researchers from different fields of science and technology to unfold more efficient diagnostic and therapeutic approaches (Xin et al. 2017). Significant solicitude has been dedicated to the

combination of nuclear medicine and nanomaterials to transfigure the conventional methods of cancer diagnosis and treatment (Silindir-Gunay and Ozer 2017; Smith and Gambhir 2017). Graphene oxide (GO) is a promising carbon family nanomaterial with rational multifunctional applications owing to its realistic physicochemical properties such as honeycomb-lattice with sp^2 hybridized carbon in two-dimensional geometry, the largest surface area for a nanoscale material and availability of various surface oxygen groups (hydroxyl, epoxides, and carboxylic groups) (Jaymand, et al. 2021; Kostas Kostarelos and Novoselov 2014; Pan et al. 2012; Smith and Gambhir 2017; Y. Yang, et al. 2012). The biocompatibility analysis of graphene-based materials is an indispensable prerequisite for in vivo biomedical applications. Hence, various studies had been explored the *in vitro* and *in vivo* cyto- and bio-compatibility declaring that graphene toxicity is highly dependent on the physiochemical properties (Lalwani et al. 2016; Yoo et al. 2015; B. Zhang et al. 2016). The size architectures, size and morphology, might affect the cellular uptake while functional groups functionalization might change the interactions with micronutrients and proteins (De Marzi, et al. 2014; H. Zhang, et al. 2013). The starting materials and production methods could evolve metallic impurities in the final product (Wong, et al. 2014). The post-synthetic treatment for providing aqueous dispersion might also influence the toxicity (Mullick Chowdhury et al. 2014). Regarding the *in vivo* toxicology and pharmacokinetics of graphene-based materials; Yang et al. explored the biodistribution behavior of PEGylated [^{125}I]iodo-labeled nanographene sheets post-intravenous injection (IV) in long-term manner demonstrating reduced radioactivity levels in most organs and tissues by time (K. Yang, et al. 2011). They also explored the blood biochemistry and hematology studies declaring non-significant toxicity for 3 months. In the past decades, chelators-based radioisotopes labeling of GO as nanotheranostics had been demonstrated but showed some predestined challenges in regard to changing the hydrophilicity, surface charge and size of the tracer (Cornelissen, et al. 2013; Hong et al. 2012a, b; Kostas Kostarelos and Novoselov 2014). Intrinsic, non-chelation, radiolabeling methods were recently employed where the radioisotopes can directly tagged-into the nanoparticles surface preserving the native physicochemical as well as *in vivo* biological behavior (Goel et al. 2014; Shi, et al. 2017; Xiaolian Sun et al. 2015). In this regard, the small thickened GO radiotracers can facilely extravasate though the leaky vasculature's body compartments (tumor and infarcts) owing to the enhanced permeability and retention (EPR) phenomena, passive targeting (Jasim, et al. 2021; Jaymand, et al. 2021). On the other hand, biological ligands can directly functionalize the oxygen-rich functional groups of GO surface for potentiating targeted drug delivery-based active targeting approach (Mohanta, et al. 2021; Zhao and Liu 2014). Folic acid (FA), a biological ligand associated with several human folate-receptors (FRs) overexpressed in many cancers, has received significant interest as a targeting candidate for cancer theranostics due to its low cost, high stability and facilely conjugated chemistry (Thapa, et al. 2016; Zhao and Liu 2014). Overall, GO-based nano-systems can facilitate the evolution of an ideological approach to scale up new technologies for tackling the detection limits of cancer's early diagnosis and improving drug targeting as well as therapy approaches. In the present study, carboxyl-functionalized GO nanosheets (FGO), passively targeted nano-formulation, with superior physicochemical characteristics were developed using an improved and eco-friendly Hummers method. These nanosheets were exposed to

amidation reaction to conjugate FA moiety compromising folate-targeting nano-formulation. The resulting two nano-formulations were appointed to chelator-free iodine-131 [^{131}I] radiolabeling in which the optimization process was fully controlled. The *in vivo* studies of both nano-theranostics in tumor-bearing mice were performed to directly appraise different targeting approaches.

Results and discussion

The synthetic procedure of CGO is depicted schematically in three steps (Fig. 1) and demonstrated as follows: synthesis of GO nanosheets, carboxyl-functionalization of GO nanosheets and conjugation of FGO with FA via amide bond formation.

Synthesis and functionalization of graphene oxide nanosheets

Improved Hummers method, an eco-friendly procedure, was utilized to synthesis graphene oxide nanosheets in which sodium nitrate was excluded during the preparation preventing the formation of harmful gases (NO_2/N_2O_4) (J. Chen et al. 2013; K. Yang et al. 2013). This method relies on the oxidizing capability of H_2SO_4 solution containing $KMnO_4$ to convert graphite to GO. The obtained yellow-colored slurry during the synthesis and the yellowish-brown color after exfoliation indicate the successful oxidation of graphite and the formation of small sized GO (J. Chen, et al. 2013; Velasco-Soto, et al. 2015; K. Yang, et al. 2013). The successful formation of GO was confirmed by the UV–visible spectrum analysis (Fig. 2A). It declared absorption peaks at 235 and 305 nm related to π–π* and n–π* transitions of C=C and C=O bonds, respectively (Noroozi et al. 2016; Romero et al. 2017). It is worth-noting that GO are rich in epoxy

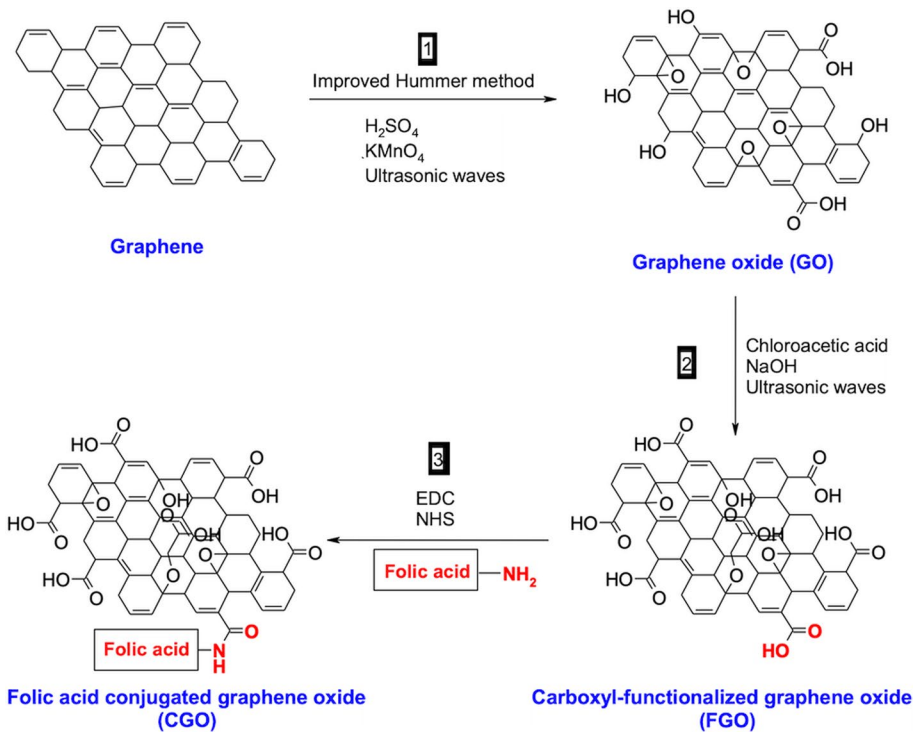

Fig. 1 Schematic illustration of the synthetic procedure of folic acid conjugated graphene oxide (CGO)

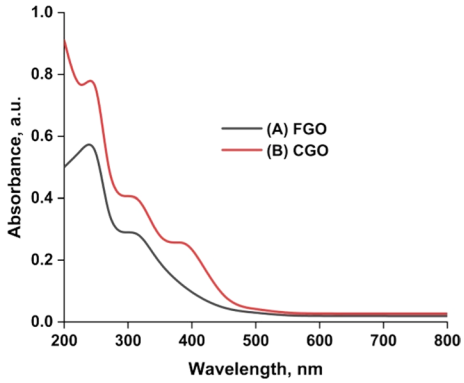

Fig. 2 UV–vis spectrum of **A** carboxyl-functionalized graphene oxide (FGO) **B** folic acid conjugated graphene oxide (CGO)

and hydroxyl groups that need to be converted to carboxyl groups for providing further functionalization/conjugation as well as improving the water solubility (Xiaoming Sun et al. 2008; L. Zhang et al. 2010). In our study, the carboxylation of graphene oxide was performed utilizing chloroacetic acid in highly basic conditions which indicated by the color change from yellowish-brown to brownish-black attributed to the partial reduction (Song and Xu 2013; Zhao and Liu 2014).

Synthesis of folate conjugated graphene oxide nanosheets (CGO)

Upon carboxylation, the affordable carboxylic groups on the GO edges could be utilized for the chemical conjugation with folic acid via amide bond formation. The amidation reaction-based EDC/NHS chemistry is a very popular procedure for the synthesis of high yield conjugates (Hermanson 2013). EDC/NHS agents have the ability to activate the carboxylic groups on the GO for straightforward reaction with the amine group of folic acid forming amide linkage nano-conjugate (Fig. 3). The successful conjugation was checked by UV–visible analysis demonstrating the appearance of a new peak at 385 nm in addition to the other two peaks related to GO (Fig. 2B). This new peak may be attributed to the pterin ring in FA (Kato, et al. 2004; Zhao & Liu 2014).

Characterization of FGO and CGO

For the morphological examination, graphene nanosheets showed a crystalline nanometric texture while conjugated graphene nanosheets showed jaggy-like texture (Fig. 4). The lateral width of CGO was 10.5–12.5 nm as one side dimension (Fig. 5). Both FGO and CGO had shown high stability nature that was confirmed with their surface zeta potential charge − 41 mV and − 34 mV, respectively.

FT-IR was performed to study the surface functional groups and to confirm the conjugation between FGO with folic acid. 1695.62 cm^{-1} in CGO confirming amide carbonyl group and 1020.08 cm^{-1} in CGO confirming C–N stretching. The broad band at 3438.10 cm^{-1} in CGO confirms carboxylic group (Fig. 6).

In vitro cytotoxicity assay

It is crucial to determine whether the developed two nanosheets have a harmful effect on the normal cells. Figure 7 demonstrates the cytotoxic profile of FGO and

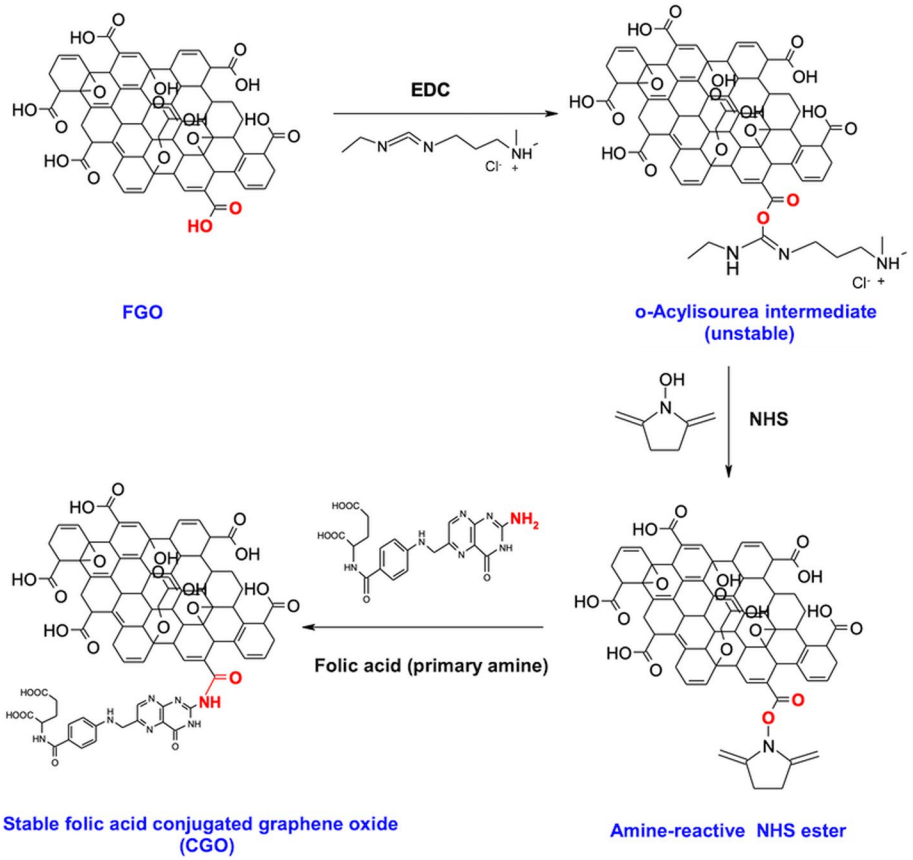

Fig. 3 Schematic illustration of the amide bond formation between FGO and FA utilizing EDC/NHS chemistry

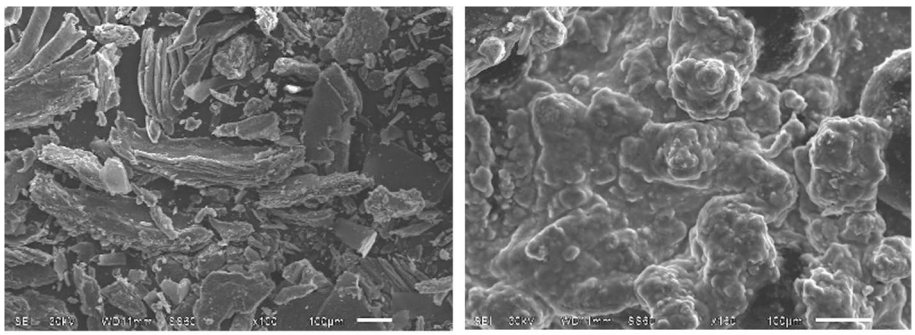

(a) **(b)**

Fig. 4 SEM images of **a** FGO and **b** CGO

CGO nanosheets against WI-38 cell line. It declared that the cells exposed to 25 µg/ml of FGO and CGO exhibited 96.94 and 100% viability level which decreased to 78.43 and 91.43% by increasing the concentration to 100 µg/ml, respectively. These results ensure that FGO as well as CGO are comparatively non-toxic to normal cells as no significant toxicity was observed, even at the highest tested concentration (100 µg/ml).This cyto-compatible behavior may be attributed to the nano-sized construction as well as carboxyl functionalization where GO toxicity extremely depends on its size

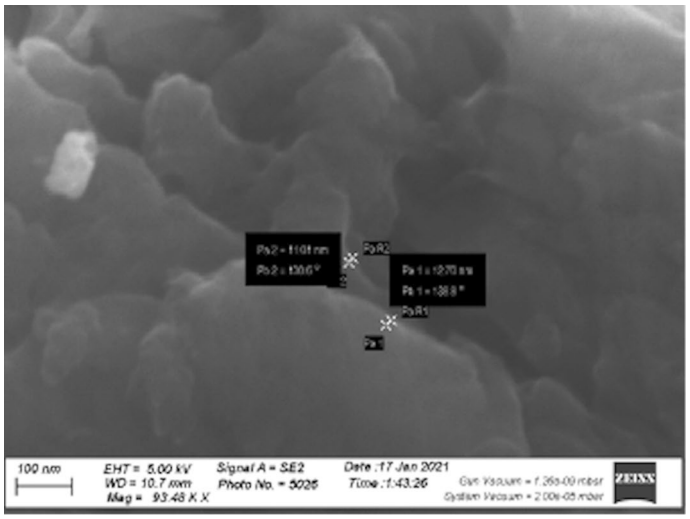

Fig. 5 SEM images of CGO lateral width

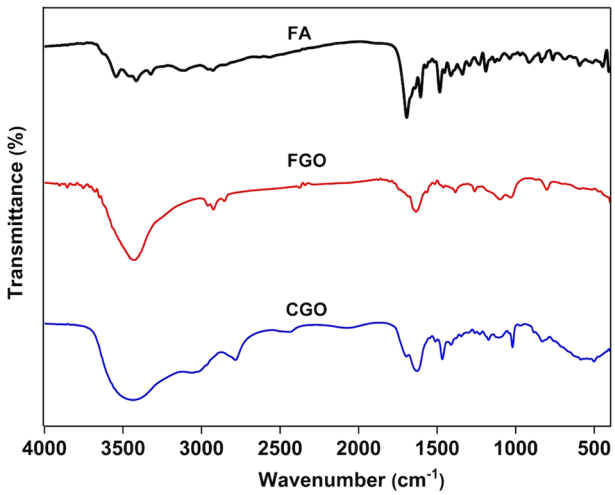

Fig. 6 FT-IR analysis of folic acid, FGO and CGO

and hydrophobicity (Burdanova et al. 2021; Muthoosamy et al. 2014; Sasidharan, et al. 2011). These results exhibited a reasonable cyto-compatibility profile that prompted further in vivo experiments. Our results are in accordance with most of the current literatures demonstrating the great biocompatibility behavior of graphene quantum dots (GQDs) (Perini et al. 2020, 2021, 2022). Shang et al. reported that GQDs showed high biocompatibility on neural stem cells even at relatively high concentrations of nanoparticles (250 μg/ml) (Shang, et al. 2014). Fasbender et al. also reported high viability of human red blood cells even after administration of GQDs at 500 μg/ml (Fasbender, et al. 2017). Moreover, Nurunnabi et al. highlighted low cytotoxicity of carboxylated GQDs at concentrations ranging from 0 to 250 μg/ml (Nurunnabi, et al. 2013). Another study investigated the effect on A549 and C6 cell lines of three different surface chemistries: carboxylation, amination and functionalization with dimethylformamide. In all cases,

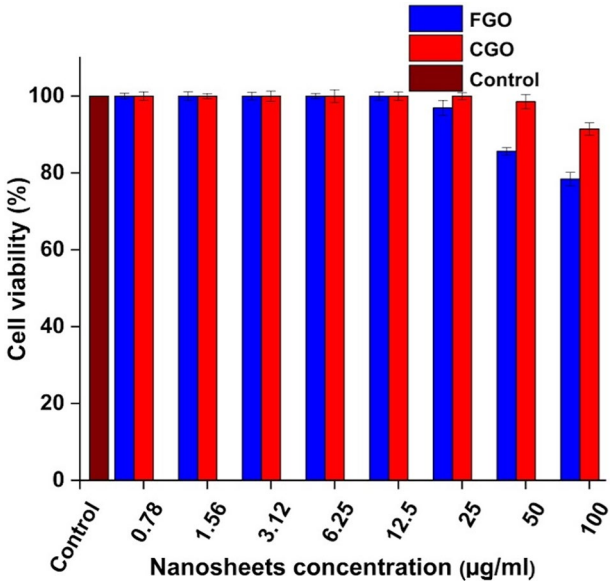

Fig. 7 Cell viability assay of FGO and CGO against WI-38 normal cells cultured 37 °C for 48 h

they measured a slight reduction in cell viability as well as a very low mortality (Yuan, et al. 2014).

Radiosynthesis of radioiodinated functionalized graphene nanosheets (IFGO) and folate conjugated graphene oxide nanosheets (ICGO)

The radiolabeling of both tracers was achieved using intrinsic radioiodination approach where the radionuclide is directly attached to the surface of the nanoparticles without the need of any chelators. The radioiodination of FGO and CGO reach their highest RCP by optimization of all parameters affecting the radioiodination process. The electrophilic substitution of iodine-131 was carried out in the presence of chloramine-T as an oxidizing agent. Iodide ion was converted to iodonium ion by the aid of Chloramine-T (Fayez et al. 2020) which has a significant impact on the radioiodination process, also it permits the occurrence of the electrophilic substitution process. Figures 8a and 9a show the optimum amount of 200 µg from CAT which create the highest RCP of 96.58% and 94.11% for [^{131}I]I-FGO and [^{131}I]I-CGO, respectively. Insufficient oxidation of I-131 and undesirable oxidative byproduct may be due to low or high amounts of CAT, respectively (Selim et al. 2021; Swidan et al. 2014). RCP also depends greatly on the pH values of the reaction mixture. The RCP was increased by increasing pH from acidic values to nearly neutral values (pH 8) and decreases by increasing pH values more than 8 as shown in Figs. 8b and 9b for [^{131}I]I-FGO and [^{131}I]I-CGO, respectively, this decrease in RCP may be due to iodate (IO_3^-) and hypoiodite (IO^-) ion formation (Saha 2012; M. Swidan et al. 2015). Figures 8c and 9c illustrate the effect of substrate amount (FGO and CGO) on the RCP, % where the highest RCP was gained at 500 µL substrate for both reaction which can capture all iodonium ion from the reaction mixture and there are no significant changes in RCP during increasing substrate amounts. The speed of this reaction and stability of the formed radioiodinated compound is shown in Figs. 8d and 9d for

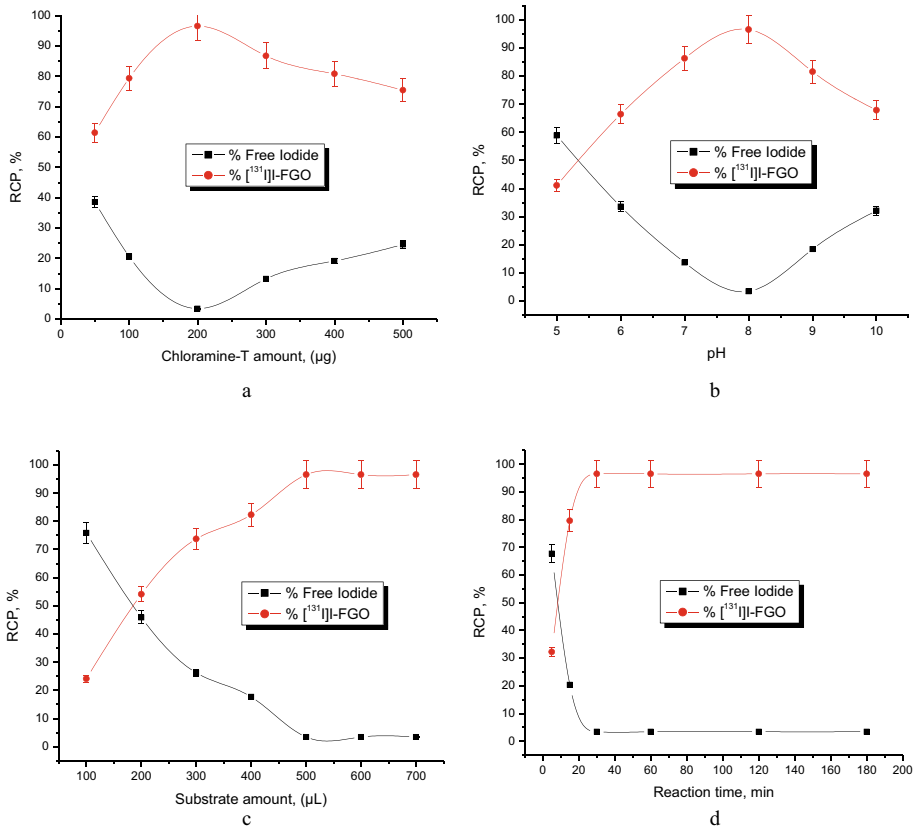

Fig. 8 Variation of RCP of [^{131}I]I-FGO as a function of variable parameters: **a**) CAT amount; **b**) pH; **c**) substrate amount; **d**) reaction time

[^{131}I]I-FGO and [^{131}I]I-CGO, respectively. The reaction was completed after 30 min and their RCP were stable for 24 h. Overall, it is worth-noting that the direct introduction of ^{131}I radionuclide to the surface of GO (intrinsic radioiodination) did not alter the physicochemical properties, size and charge characteristics, of the native preparation based on the re-characterization analysis beyond the full radioactive decay (~ 10 half-lives). This superior intrinsic radioiodination might introduce the priority of our developed radiotracers over the previously published ones synthesized by the chelator-based radiolabeling (Cornelissen, et al. 2013; Hong et al. 2012a, b; D. Yang, et al. 2016). For example, Cornelissen et al. demonstrated the radiolabeling of GO with indium-111 [^{111}In] through diethylenetriaminepentaacetic acid (DTPA) chelating agent strategy revealing dramatic increase in the thickness of the GO sheets (Cornelissen, et al. 2013).

Biological evaluation of radioiodinated functionalized graphene nanosheets (IFGO) in normal mice model

IFGO showed a typical biodistribution behavior as a nanomaterial (Fig. 10). It was washed out from blood in a good behavioral way with a decrease from 16.35 ± 1.54 to 3.21 ± 0.14%ID/g at 30 min and 150 min, respectively. Three main organs represented the targeted organs of nanoparticles; Liver, spleen and lungs. The highest uptake %ID/g of liver (13.68 ± 1.56), spleen (6.07 ± 1.01) and lungs (9.69 ± 1.21) was observed at

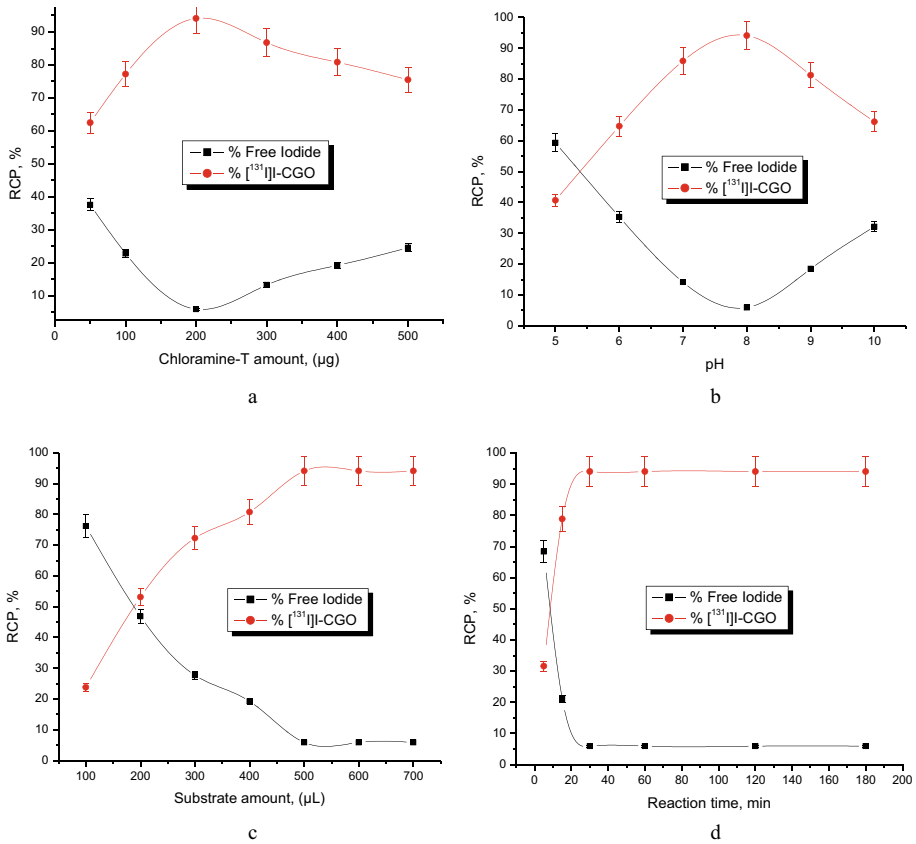

Fig. 9 Variation of RCP of [^{131}I]I-CGO as a function of variable parameters: **a**) CAT amount; **b**) pH; **c**) substrate amount; **d**) Reaction time

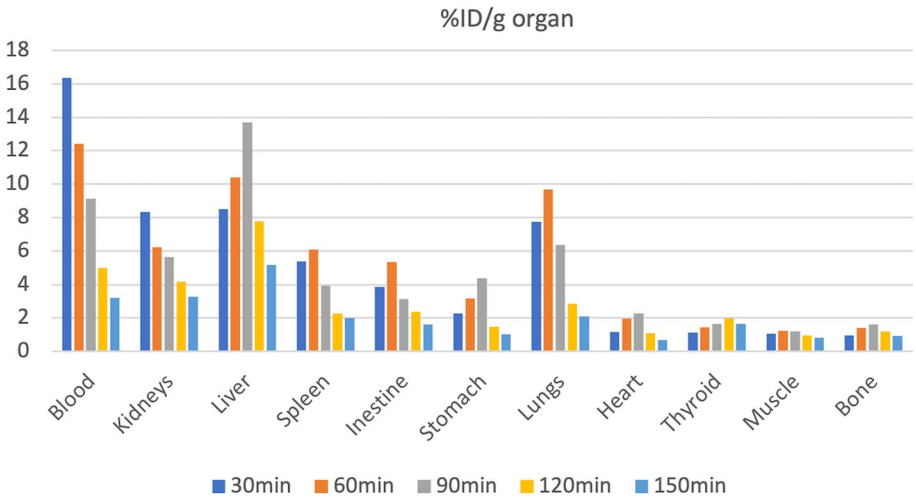

Fig. 10 Normal biodistribution behavior of radioiodinated functionalized carbon nanosheets (IFGO) in normal mice model as a function of %ID/g organ

90 min, 60 min, 60 min, respectively. Hepatobiliary and renal pathways were the main excretory ways of IFGO as shown in the uptake %ID/g of liver, kidneys and intestine. Renal pathway was the fastest excretory route as kidneys showed 8.32 ± 1.83%ID/g at

30 min. All other body organs did not show any valuable accumulation of IFGO. The *in vivo* distribution behavior of IFGO in normal mice was matched with the biodistribution of almost carbon-based radiolabeled nanomaterials (Jaymand, et al. 2021; K Kostarelos et al. 2009). Wei et al. investigated the in vivo biodistribution of technetium-99m labeled oxidized multi-walled carbon nanotubes (^{99m}Tc labeled oMWCNTs) declaring that the radiotracer was mostly accumulated in liver, spleen and lungs (Wei, et al. 2012). Menezes et al. fabricated GQDs through a green chemistry approach and labeled them with ^{99m}Tc. They reported very limited off-target uptake by the mononuclear phagocytic system and the organ biodistribution in healthy animals (De Menezes, et al. 2019). Additionally, Yang et al. explored the long-term in vivo biodistribution of ^{125}I-labeled nanographene sheets (NGS) functionalized with polyethylene glycol (PEG) revealing main accumulation in the reticuloendothelial system (RES) including liver and spleen after intravenous administration and can be gradually cleared, likely by both renal and fecal excretion (K. Yang, et al. 2011).

In vivo comparative study between radioiodinated functionalized graphene nanosheets (IFGO) and radioiodinated conjugated graphene nanosheets (ICGO) in tumor-bearing mice model

Figure 11 confirms efficient selectivity of ICGO to target tumor tissues in huge advance than IFGO. By deep analysis of the uptake %ID/g of the main important organs, liver, spleen, lungs and tumor, it is so clear that after the conjugation of functionalized graphene nanosheets with folic acid, liver, spleen and lungs uptakes %ID/g intensively decreased with impressive increase of tumor uptake %ID/g. Additionally, the folate-receptors tumor targeted radiotracer, IFGO, demonstrated maximum tumor accumulation (~14%ID/g) representing a superior prominence over the previously published tumor targeted, vascular endothelial growth factor receptor (VEGFR) and follicle stimulating hormone receptor (FSHR), GO radiotracers with potential tumor uptake ~8 and 11.5%ID/g, respectively (Shi, et al. 2015; D. Yang, et al. 2016).

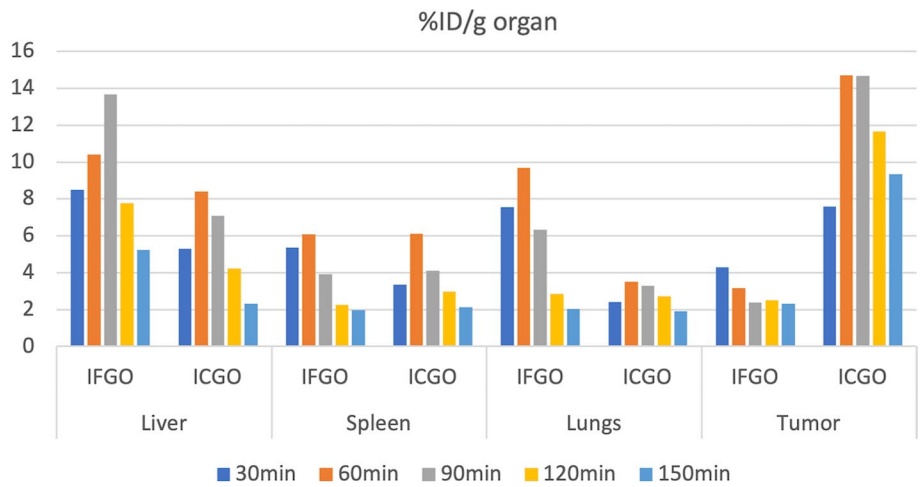

Fig. 11 Uptake %ID/g organ (liver, spleen, lungs and tumor) of radioiodinated functionalized graphene nanosheets (IFGO) and radioiodinated conjugated graphene nanosheets (ICGO) in tumor-bearing mice mode

Target/nontarget ratio represents the uptake %ID/g organ of tumor muscle/normal muscle that confirms the selectivity of the injected agent for differentiating between cancer and normal cells from the same tissue origin (Mahmoud et al. 2022). As presented in Fig. 12, it is clear that T/NT of ICGO (7.27 and 7.19 at 60 min and 90 min, respectively) showing in average 4–5 times folds of T/NT of IFGO (1.9 and 1.56 at 60 min and 90 min, respectively). Furthermore, our synthesized radiotracer (IFGO) demonstrated higher tumor accumulation with lower RES-organs' uptakes when compared to ^{131}I-labeled PEG-functionalized reduced nano-GO (^{131}I-RGO-PEG) (L. Chen, et al. 2015). IFGO showed a significant reduction in accumulation within the spleen, liver, and lung when compared to amino-functionalized GO labelled with radioactive gold nanoparticles (^{198,199}Au-labeled amino-functionalized GO) as a SPECT imaging and therapeutic agent (Fazaeli et al. 2014).

Methods

Chemicals and equipment

The natural graphite powder (99.9%), potassium permanganate ($KMnO_4$, 95%), concentrated sulfuric acid (H_2SO_4, 98%), hydrochloric acid (HCl, 37%), hydrogen peroxide (H_2O_2, 37%), sodium hydroxide (NaOH, > 98%), chloroacetic acid ($ClCH_2COOH$, 99%), N-(3-dimethylaminopropyl-N'-ethylcarbodiimide) hydrochloride, EDC ($C_8H_{17}N_3$·xHCl), N-Hydroxysuccinimide, NHS ($C_4H_5NO_3$, 98%), Dimethyl sulfoxide, DMSO ($(CH_3)_2SO$, > 99%), folic acid ($C_{19}H_{19}N_7O_6$, > 97%), Dulbecco's minimum essential medium (DMEM), fetal bovine serum (FBS) as well as MF-Millipore® Membrane Filter (0.22 µm pore size) were purchased from Sigma-Aldrich company (Darmstadt, Germany). All solutions preparation as well as sanitation processes were performed utilizing ultrapure water (a Milli-Q purification system (Merck, Massachusetts, USA). Shimadzu UV-1700 spectrophotometer (Thermo Fisher Scientific, USA) geared up with 1 cm quartz optical length cuvettes was applied to confirm the proper formation of the nanosheets. Ultrasonic bath P30H (Elma Schmidbauer GmbH, Germany) operating at 200 W was applied for dispersion purposes. Photo correlation spectrometer (PCS) was used using Brookhaven 90 plus (Zetasizer Nano™, Beckman Coulter, Miami, FL, USA).

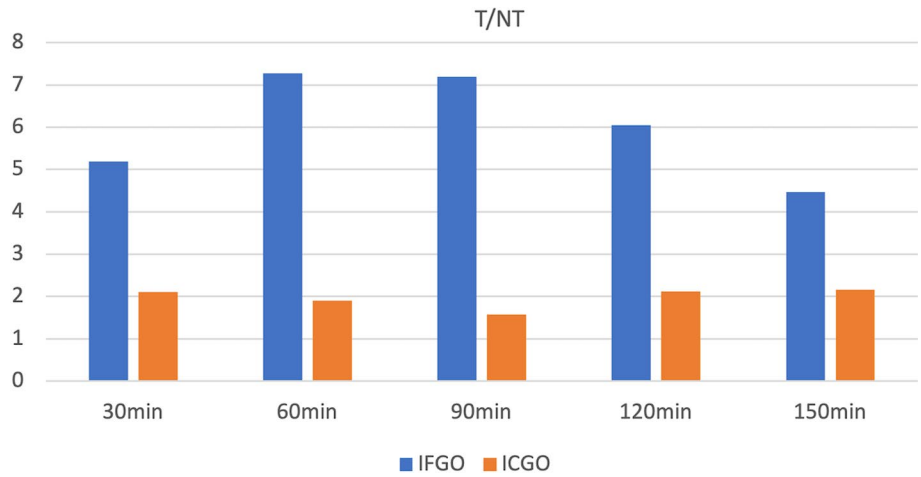

Fig. 12 Target/nontarget (T/NT) of IFGO and ICGO in tumor-bearing mice model

UV–visible Spectroscopy was performed using a Cyber lab UV-100 double beam spectrophotometer (Thermo Fisher Scientific, USA). Fourier transform infrared (FT-IR) spectra were obtained on Perkin Elmer Spectrum 100 Spectrometer (Mattson Instruments, Inc., New Mexico, USA). No-carrier-added [^{131}I]NaI was received as a gift from RPF (Radioisotopes-Production-Facility), Egyptian Atomic Energy Authority (EAEA). A NaI (Tl) scintillation counter (Scaler Ratemeter SR7 model, the United Kingdom) was used for γ-ray radioactivity measurement. Thin layer chromatography (TLC) was carried out on the plates of silica gel (Merck Kiesel gel 60F254, BDH) to monitor the progress of the radiosynthesis process.

Synthesis and functionalization of graphene nanosheets (FGO)

Graphene oxide nanosheets (GO) were synthesized according to an improved Hummers method (J. Chen, et al. 2013; K. Yang, et al. 2013). Briefly, the natural graphite powder (1 g) was dissolved in a concentrated solution of sulfuric acid (23 ml) under vigorous magnetic stirring in an ice-bath. This is followed by slow addition of potassium permanganate (3 g) in which the reaction temperature should not exceed 20 °C. The suspension flask was moved into a water bath at 40 °C and vigorously stirred for 30 min. Then, the reaction temperature was raised to 70 °C in which the suspension color changed to brown. Subsequently, a definite volume of water (50 ml) was slowly added and the reaction proceeded at 95 °C for 15 min followed by another addition of 150 ml of water. Next, hydrogen peroxide (10 ml) was added turning the dispersion color to yellow, which indicates the formation of GO nanosheets. Finally, the purification process was performed through centrifuging the dispersion at 12,000 rpm for 20 min followed by washing the resultant precipitate with 10 ml hydrochloric acid (10% *v/v*) to remove the metal ions and then water washing was utilized until neutral pH was achieved. The GO aqueous dispersion was exfoliated by 60 min bath-sonication process to obtain small nano-sized flaks. The exfoliated dispersion was centrifuged for 15 min at 12000 rpm in order to remove the un-exfoliated flaks. The carboxylic acid functionalization of GO was performed according to previous literatures (Song & Xu 2013; K. Yang, et al. 2011). Sodium hydroxide (0.12 g/ml) and chloroacetic acid (0.1 g/ml) were fully dissolved in an aqueous dispersion of GO (2 mg/ml, 10 ml). This mixture was forced for 3 h bath-sonication. The resulting mixture was neutralized with dilute hydrochloric acid and purified by repeated rinsing and filtration until well dispersion (carboxyl-functionalized graphene oxide (FGO) was obtained.

Synthesis of folate conjugated graphene oxide nanosheets (CGO)

Folic acid (FA) was conjugated to carboxylated graphene oxide through covalent bond formation between the carboxyl groups of FGO and the amine group of FA (Eivazzadeh-Keihan, et al. 2022; Qin, et al. 2013). Briefly, a definite concentration of EDC and NHS (5 mg/ml and 1 mg/ml, respectively) were added to the dispersion of FGO in DMSO (1 mg/ml) and then the mixture was sonicated for 30 min. Another portion of EDC was further added while the sonication continues for another 30 min. Then, FA (2 mg/ml) was added and the mixture was preceded under stirring overnight at room temperature. Finally, the mixture was centrifuged and washed twice with water and ethanol to get rid of excess DMSO as well as any unconjugated FA. The mixture was filtered using 0.22 μm

membrane filter and then the product (folate conjugated graphene oxide; CGO) was re-dispersed in water for washing and then filtered again, left for air-drying then collected.

Characterization of FGO and CGO

The morphological appearances, sizes and surface charges of both of functionalized graphene nanosheets and conjugated graphene nanosheets were evaluated using SEM and PCS instruments. FT-IR analysis was performed for free folic acid, functionalized graphene nanosheets (FGO) and conjugated graphene nanosheets (CGO) to evaluate the surface function groups and confirm the conjugation between folic acid and functionalized graphene nanosheets.

In vitro cytotoxicity assay

Normal human lung fibroblast cell line (WI-38 cells) that deposited overnight on 96-well plates (4000/well) were refined using Dulbecco's modified Eagle's medium (DMEM) loaded with 10% fetal bovine serum, 1% streptomycin–penicillin antibiotics. The cells were then cultivated at 37 °C for 48 h in a 5% CO_2 saturated humid incubator in the presence of different concentrations of FGO as well as CGO. Control cell line was assessed without incorporating any of the tested samples. After the incubation period was complete, the cell growth was spectrophotometrically analyzed to identify the absorbance of the plates with the help of crystal violet solution (1%) at tested wavelength 490 nm.

Radiosynthesis of radioiodinated functionalized graphene nanosheets (IFGO) and radioiodinated folate conjugated graphene oxide nanosheets (ICGO)

Radioiodination procedure was carried out by studying different amounts for both the synthesized FGO and CGO (100–700 µL) solutions, then (50–500 µg) of freshly prepared chloramine-T (CAT) solution were added. After that, 10 µL of [^{131}I]NaI (4 MBq) was added to the mixture of the reactions, and the pH values were adjusted from 5 to 10. The reactions were kept at room temperature up to 24 h. After a definite time, the reactions were quenched using sodium metabisulphite solution. All these parameters were carefully studied in order to obtain the highest radiochemical purity (RCP). Formation of [^{131}I]I-FGO and [^{131}I]I-CGO were monitored by using TLC using methanol (70%). 2 µL from each reaction mixture was spotted at a point of 2 cm from lower edge of TLC paper strip (13 cm length and 1 cm width), then the strip was developed ascendingly in a closed glass tube containing a freshly prepared methanol (70%) as a mobile phase. free iodide was migrate with the solvent at $R_f = 0.7–1$; while [^{131}I]I-FGO and [^{131}I]I-CGO remained at origin ($R_f = 0–0.1$), then the RCP was calculated. After reaction completion both [^{131}I]I-FGO and [^{131}I]I-CGO were purified from free iodine using TLC technique.

Biological evaluation of radioiodinated functionalized graphene nanosheets (IFGO) in normal mice model

Radioiodinated functionalized graphene nanosheets (IFGO) were evaluated in vivo in normal mice model to determine its biodistribution behavior with different time intervals (30, 60, 90, 120 and 150 min). The different percentage injected dose per gram (%ID/g) values for each organ and fluid were calculated ex vivo after extracting all mice parts at the assigned time points (El-Ghareb, et al. 2020; Sakr, et al. 2018; M. M. Swidan,

et al. 2019). Three mice were examined at each time point. Statistical evaluation for the results was applied. All the approvals for ethics regulations were obtained from Egyptian Atomic Energy Authority.

In vivo comparative study between radioiodinated functionalized graphene nanosheets (IFGO) and radioiodinated conjugated graphene nanosheets (ICGO) in tumor-bearing mice model

IFGO and ICGO were evaluated in vivo in tumor-bearing mice model to determine their accumulation in tumor tissues besides the relevant organs such as lung, liver, spleen and normal muscle. Tumor was induced in right thigh muscle of mice using Ehrlich ascites carcinoma obtained from the National Cancer institute, Egypt. Mice selected organs were collected and evaluated for %ID/g to compare between the targeting ability of both agents in vivo and to evaluate their retaining ability in the other relevant organs (Aljuhr et al. 2021; Essa et al. 2020; Sakr et al. 2020).

Conclusion

The presented work succeeded to develop two different potential non-toxic nano-radiopharmaceutical agents based on graphene oxide nanosheets that were able to target cancer tissues selectively either passively or actively. It was also proven that the decoration of these graphene oxide nanosheets with selective tumor targeting moiety intensively enhances its tumor targeting ability and accordingly uptake and retention. This preliminary study highlights the usefulness of using such a multifunctional agent to image and treat tumor tissues.

Abbreviations

GO	Graphene oxide nanosheets
FA	Folic acid
FGO	Functionalized graphene oxide nanosheets
CGO	Conjugated graphene oxide nanosheets
IFGO	Radioiodinated functionalized graphene oxide nanosheets
ICGO	Radioiodinated conjugated graphene oxide nanosheets
NHS	N-Hydroxysuccinimide
EDC	N-(3-Dimethylaminopropyl-N′-ethylcarbodiimide) hydrochloride
RCP	Radiochemical purity
DMSO	Dimethyl sulfoxide
TLC	Thin layer chromatography
CAT	Chloramine-T
MBq	Megabecquerel
Rf	Retention factor
VEGFR	Vascular endothelial growth factor receptor
FSHR	Follicle stimulating hormone receptor
DTPA	Diethylenetriaminepentaacetic acid

Acknowledgements

This paper is based upon work supported by The Science, Technology & Innovation Funding Authority (STDF)—Applied Science Research Grants ID 46045, Cairo, EGYPT.

Author contributions

All authors read and approved the final manuscript.

Funding

Open access funding provided by The Science, Technology & Innovation Funding Authority (STDF) in cooperation with The Egyptian Knowledge Bank (EKB).

Availability of data and materials
All data generated or analyzed during this study are included in this published article.

Declarations

Ethics approval and consent to participate
All experimental protocols were approved by the Egyptian Atomic Energy Authority animal ethics committee protocol number (215/20-04-2022) which follows the principles of European Community guidelines associated with Directive 2010/63/EU on the protection of animals used for scientific purposes. This study was conducted in accordance with the ARRIVE guidelines (https://arriveguidelines.org).

Consent for publication
Not applicable.

Competing interests
The authors declare that they have no competing interests.

Received: 1 November 2022 Accepted: 22 January 2023
Published online: 02 February 2023

References

Aljuhr SA, Abdelaziz G, Essa BM, Zaghary WA, Sakr TM (2021) Hepatoprotective, antioxidant and anti-inflammatory potentials of Vit-E/C@ SeNPs in rats: synthesis, characterization, biochemical, radio-biodistribution, molecular and histopathological studies. Bioorg Chem 117:105412
Burdanova MG, Kharlamova MV, Kramberger C, Nikitin MP (2021) Applications of pristine and functionalized carbon nanotubes, graphene, and graphene nanoribbons in biomedicine. Nanomaterials 11(11):3020
Chen J, Yao B, Li C, Shi G (2013) An improved Hummers method for eco-friendly synthesis of graphene oxide. Carbon 64:225–229
Chen L, Zhong X, Yi X, Huang M, Ning P, Liu T et al (2015) Radionuclide 131I labeled reduced graphene oxide for nuclear imaging guided combined radio-and photothermal therapy of cancer. Biomaterials 66:21–28
Cornelissen B, Able S, Kersemans V, Waghorn PA, Myhra S, Jurkshat K et al (2013) Nanographene oxide-based radioimmunoconstructs for in vivo targeting and SPECT imaging of HER2-positive tumors. Biomaterials 34(4):1146–1154
De Marzi L, Ottaviano L, Perrozzi F, Nardone M, Santucci S, De Lapuente J et al (2014) Flake size-dependent cyto and genotoxic evaluation of graphene oxide on in vitro A549, CaCo2 and vero cell lines. J Biol Regul Homeost Agents 28(2):281–289
Duarte F, de Menezes S, Rezende R, dos Reis S, Pinto R, Portilho FL, do ChavesMello FV, Helal-Neto E et al (2019) Graphene quantum dots unraveling: Green synthesis, characterization, radiolabeling with 99mTc, in vivo behavior and mutagenicity. Mater Sci Eng 102(405):414
Eivazzadeh-Keihan R, Alimirzaloo F, Aliabadi AM, BahojbNoruzi HE, Akbarzadeh AR, Maleki A et al (2022) Functionalized graphene oxide nanosheets with folic acid and silk fibroin as a novel nanobiocomposite for biomedical applications. Sci Rep 12(1):1–12
El-Ghareb WI, Swidan MM, Ibrahim IT, Abd El-Bary A, Tadros MI, Sakr TM (2020) 99mTc-Doxorubicin-loaded gallic acid-gold nanoparticles (99mTc-DOX-loaded GA-Au NPs) as a multifunctional theranostic agent. Int J Pharm 586:119514
Essa BM, El-Mohty AA, El-Hashash MA, Sakr TM (2020) 99mTc-citrate-gold nanoparticles as a tumor tracer: synthesis, characterization, radiolabeling and in-vivo studies. Radiochim Acta 108(10):809–819
Fasbender S, Allani S, Wimmenauer C, Cadeddu R-P, Raba K, Fischer JC et al (2017) Uptake dynamics of graphene quantum dots into primary human blood cells following in vitro exposure. RSC Adv 7(20):12208–12216
Fayez H, El-Motaleb MA, Selim AA (2020) Synergistic cytotoxicity of shikonin-silver nanoparticles as an opportunity for lung cancer. J Labelled Compd Radiopharm 63(1):25–32
Fazaeli Y, Akhavan O, Rahighi R, Aboudzadeh MR, Karimi E, Afarideh H (2014) In vivo SPECT imaging of tumors by 198,199 Au-labeled graphene oxide nanostructures. Mater Sci Eng, C 45:196–204
Goel S, Chen F, Ehlerding EB, Cai W (2014) Intrinsically radiolabeled nanoparticles: an emerging paradigm. Small 10(19):3825–3830
Hermanson GT (2013) Bioconjugate techniques. Academic press, Cambridge
Hong H, Yang K, Zhang Y, Engle JW, Feng L, Yang Y et al (2012a) In vivo targeting and imaging of tumor vasculature with radiolabeled, antibody-conjugated nanographene. ACS Nano 6(3):2361–2370
Hong H, Zhang Y, Engle JW, Nayak TR, Theuer CP, Nickles RJ et al (2012b) In vivo targeting and positron emission tomography imaging of tumor vasculature with 66Ga-labeled nano-graphene. Biomaterials 33(16):4147–4156
Jasim DA, Newman L, Rodrigues AF, Vacchi IA, Lucherelli MA, Lozano N et al (2021) The impact of graphene oxide sheet lateral dimensions on their pharmacokinetic and tissue distribution profiles in mice. J Control Release 338:330–340
Jaymand M, Taghipour YD, Rezaei A, Derakhshankhah H, Abazari MF, Samadian H et al (2021) Radiolabeled carbon-based nanostructures: new radiopharmaceuticals for cancer therapy? Coord Chem Rev 440:213974
Kato T, Matsuoka T, Nishii M, Kamikawa Y, Kanie K, Nishimura T et al (2004) Supramolecular chirality of thermotropic liquid-crystalline folic acid derivatives. Angew Chem Int Ed 43(15):1969–1972
Kostarelos K, Novoselov KS (2014) Exploring the interface of graphene and biology. Science 344(6181):261–263
Kostarelos K, Bianco A, Prato M (2009) Promises, facts and challenges for carbon nanotubes in imaging and therapeutics. Nat Nanotechnol 4(10):627–633

Lalwani G, D'Agati M, Khan AM, Sitharaman B (2016) Toxicology of graphene-based nanomaterials. Adv Drug Deliv Rev 105:109–144
Mahmoud AF, Aboumanei MH, Abd-Allah WH, Swidan MM, Sakr TM (2022) New frontier radioiodinated probe based on in-silico resveratrol repositioning for microtubules dynamic targeting. Int J Radiat Biol. https://doi.org/10.1080/09553002.2022.2078001
Mohanta YK, Biswas K, Rauta PR, Mishra AK, De D, Hashem A et al (2021) Development of graphene oxide nanosheets as potential biomaterials in cancer therapeutics: an in-vitro study against breast cancer cell line. J Inorg Organomet Polym Mater 31(11):4236–4249
Mullick Chowdhury S, Dasgupta S, McElroy AE, Sitharaman B (2014) Structural disruption increases toxicity of graphene nanoribbons. J Appl Toxicol 34(11):1235–1246
Muthoosamy K, Bai R, Manickam S (2014) Graphene and graphene oxide as a docking station for modern drug delivery system. Curr Drug Deliv 11(6):701–718
Noroozi M, Zakaria A, Radiman S, Abdul Wahab Z (2016) Environmental synthesis of few layers graphene sheets using ultrasonic exfoliation with enhanced electrical and thermal properties. PLoS ONE 11(4):e0152699
Nurunnabi M, Khatun Z, Huh KM, Park SY, Lee DY, Cho KJ et al (2013) In vivo biodistribution and toxicology of carboxylated graphene quantum dots. ACS Nano 7(8):6858–6867
Pan Y, Sahoo NG, Li L (2012) The application of graphene oxide in drug delivery. Expert Opin Drug Deliv 9(11):1365–1376
Perini G, Palmieri V, Ciasca G, De Spirito M, Papi M (2020) Unravelling the potential of graphene quantum dots in biomedicine and neuroscience. Int J Mol Sci 21(10):3712
Perini G, Palmieri V, Ciasca G, Primiano A, Gervasoni J, De Spirito M, Papi M (2021) Functionalized graphene quantum dots modulate malignancy of glioblastoma multiforme by downregulating neurospheres formation. C 7(1):4. https://doi.org/10.3390/c7010004
Perini G, Rosa E, Friggeri G, Di Pietro L, Barba M, Parolini O et al (2022) INSIDIA 2 0 high-throughput analysis of 3d cancer models: multiparametric quantification of graphene quantum dots photothermal therapy for glioblastoma and pancreatic cancer. Int J Mol Sci 23(6):3217
Qin X, Guo Z, Liu Z, Zhang W, Wan M, Yang B (2013) Folic acid-conjugated graphene oxide for cancer targeted chemo-photothermal therapy. J Photochem Photobiol, B 120:156–162
Romero UAM, Soto MÁV, Jiménez LL, Quintana JÁ, García SAP (2017) Graphene derivatives: controlled properties, nanocomposites, and energy harvesting applications graphene materials-structure properties and modifications. IntechOpen, Londan
Saha GB (2012) Physics and radiobiology of nuclear medicine. Springer Science Business Media, Berlin
Sakr TM, Khowessah O, Motaleb M, Abd El-Bary A, El-Kolaly M, Swidan MM (2018) I-131 doping of silver nanoparticles platform for tumor theranosis guided drug delivery. Eur J Pharm Sci 122:239–245
Sakr TM, El-Hashash M, El-Mohty A, Essa BM (2020) 99mTc-gallic-gold nanoparticles as a new imaging platform for tumor targeting. Appl Radiat Isot 164:109269
Sasidharan A, Panchakarla L, Chandran P, Menon D, Nair S, Rao C et al (2011) Differential nano-bio interactions and toxicity effects of pristine versus functionalized graphene. Nanoscale 3(6):2461–2464
Selim AA, Essa BM, Abdelmonem IM, Amin MA, Sarhan MO (2021) Extraction, purification and radioiodination of Khellin as cancer theranostic agent. Appl Radiat Isot 178:109970
Shang W, Zhang X, Zhang M, Fan Z, Sun Y, Han M et al (2014) The uptake mechanism and biocompatibility of graphene quantum dots with human neural stem cells. Nanoscale 6(11):5799–5806
Shi S, Yang K, Hong H, Chen F, Valdovinos HF, Goel S et al (2015) VEGFR targeting leads to significantly enhanced tumor uptake of nanographene oxide in vivo. Biomaterials 39:39–46
Shi S, Xu C, Yang K, Goel S, Valdovinos HF, Luo H et al (2017) Chelator-free radiolabeling of nanographene: breaking the stereotype of chelation. Angew Chem Int Ed 56(11):2889–2892
Silindir-Gunay M, Ozer AY (2017) Nanosized drug delivery systems as radiopharmaceuticals nanostructures for cancer therapy. Elsevier, Amsterdam
Smith BR, Gambhir SS (2017) Nanomaterials for in vivo imaging. Chem Rev 117(3):901–986
Song M, Xu J (2013) Preparation of polyethylenimine-functionalized graphene oxide composite and its application in electrochemical ammonia sensors. Electroanalysis 25(2):523–530
Sun X, Liu Z, Welsher K, Robinson JT, Goodwin A, Zaric S et al (2008) Nano-graphene oxide for cellular imaging and drug delivery. Nano Res 1(3):203–212
Sun X, Cai W, Chen X (2015) Positron emission tomography imaging using radiolabeled inorganic nanomaterials. Acc Chem Res 48(2):286–294
Swidan M, Sakr T, Motaleb M, El-Bary AA, El-Kolaly M (2014) Radioiodinated acebutolol as a new highly selective radiotracer for myocardial perfusion imaging. J Labelled Compd Radiopharm 57(10):593–599
Swidan M, Sakr T, Motaleb M, El-Bary A, El-Kolaly M (2015) Preliminary assessment of radioiodinated fenoterol and reproterol as potential scintigraphic agents for lung imaging. J Radioanal Nucl Chem 303(1):531–539
Swidan MM, Khowessah OM, El-Motaleb MA, El-Bary AA, El-Kolaly MT, Sakr TM (2019) Iron oxide nanoparticulate system as a cornerstone in the effective delivery of Tc-99 m radionuclide: a potential molecular imaging probe for tumor diagnosis. DARU J Pharmaceutical Sci 27(1):49–58
Thapa RK, Choi JY, Poudel BK, Choi H-G, Yong CS, Kim JO (2016) Receptor-targeted, drug-loaded, functionalized graphene oxides for chemotherapy and photothermal therapy. Int J Nanomed 11:2799
Velasco-Soto M, Pérez-García S, Alvarez-Quintana J, Cao Y, Nyborg L, Licea-Jiménez L (2015) Selective band gap manipulation of graphene oxide by its reduction with mild reagents. Carbon 93:967–973
Wei Q, Zhan L, Juanjuan B, Jing W, Jianjun W, Taoli S et al (2012) Biodistribution of co-exposure to multi-walled carbon nanotubes and nanodiamonds in mice. Nanoscale Res Lett 7(1):1–9
Wong CHA, Sofer Z, Kubešová M, Kučera J, Matějková S, Pumera M (2014) Synthetic routes contaminate graphene materials with a whole spectrum of unanticipated metallic elements. Proc Natl Acad Sci 111(38):13774–13779
Xin Y, Huang M, Guo WW, Huang Q, Jiang G (2017) Nano-based delivery of RNAi in cancer therapy. Mol Cancer 16(1):1–9

Yang K, Wan J, Zhang S, Zhang Y, Lee S-T, Liu Z (2011) In vivo pharmacokinetics, long-term biodistribution, and toxicology of PEGylated graphene in mice. ACS Nano 5(1):516–522
Yang Y, Zhang YM, Chen Y, Zhao D, Chen JT, Liu Y (2012) Construction of a graphene oxide based noncovalent multiple nanosupramolecular assembly as a scaffold for drug delivery. Chem Eur J 18(14):4208–4215
Yang K, Feng L, Hong H, Cai W, Liu Z (2013) Preparation and functionalization of graphene nanocomposites for biomedical applications. Nat Protoc 8(12):2392–2403
Yang D, Feng L, Dougherty CA, Luker KE, Chen D, Cauble MA et al (2016) In vivo targeting of metastatic breast cancer via tumor vasculature-specific nano-graphene oxide. Biomaterials 104:361–371
Yoo JM, Kang JH, Hong BH (2015) Graphene-based nanomaterials for versatile imaging studies. Chem Soc Rev 44(14):4835–4852
Yuan X, Liu Z, Guo Z, Ji Y, Jin M, Wang X (2014) Cellular distribution and cytotoxicity of graphene quantum dots with different functional groups. Nanoscale Res Lett 9(1):1–9
Zhang L, Xia J, Zhao Q, Liu L, Zhang Z (2010) Functional graphene oxide as a nanocarrier for controlled loading and targeted delivery of mixed anticancer drugs. Small 6(4):537–544
Zhang H, Peng C, Yang J, Lv M, Liu R, He D et al (2013) Uniform ultrasmall graphene oxide nanosheets with low cytotoxicity and high cellular uptake. ACS Appl Mater Interfaces 5(5):1761–1767
Zhang B, Wang Y, Zhai G (2016) Biomedical applications of the graphene-based materials. Mater Sci Eng, C 61:953–964
Zhao X, Liu P (2014) Biocompatible graphene oxide as a folate receptor-targeting drug delivery system for the controlled release of anti-cancer drugs. RSC Adv 4(46):24232–24239

Publisher's Note